Brazilian Journal of Geophysics
Brazilian Geophysical Society
ISSN 2764-8044
DOI: 10.22564/brjg.v43i3.2348

SPECTRAL DECOMPOSITION AND 4D SEISMIC ATTRIBUTES ANALYSIS FOR RESERVOIR MANAGEMENT: A BRAZILIAN PRE-SALT CARBONATE CASE STUDY

Diego Chagas Garcia[1]*, Mario Paiva[2], Matheus Stanfoca Casagrande[1], Juliana Jannuzzi[2], Alexandre Rodrigo Maul[1], and Webe João Mansur[3]

Garcia, D.C. - https://orcid.org/0009-0004-3552-2762
Paiva, M.F.B - https://orcid.org/0000-0001-7949-8558
Casagrande, M.F.S. - https://orcid.org/0000-0003-2203-1652
Jannuzzi, J - https://orcid.org/0009-0008-8360-258X
Maul, A.R. - https://orcid.org/0000-0002-3556-3140
Mansur, W.J. - https://orcid.org/0000-0001-6033-9653

[1]Petróleo Brasileiro S.A. – Petrobras, Rio de Janeiro, RJ, Brazil
[2]Schlumberger Serviços de Petróleo Ltda. SLB, Rio de Janeiro, RJ, Brazil
[3]Universidade Federal do Rio de Janeiro - UFRJ Rio de Janeiro, RJ, Brazil

*Corresponding author e-mail: diegocgarcia@petrobras.com.br

ABSTRACT. Detecting 4D anomalies in pre-salt carbonate reservoirs can be a major challenge for seismic interpretation due to low impedance contrasts and complex fluid substitution effects, as those observed in Mero field located at Santos Basin, Brazil. To overcome this task, the applied methodology comprised the use of Generalized Spectral Decomposition (GSD) jointly with a 4D seismic inversion to analyze frequency, phase and the acoustic components of the 4D signal near an injector well, where frequencies (9 Hz, 18 Hz, and 26 Hz) and phase rotations (±180º, ±90º, 0º) were evaluated. The results indicate that, although the individual spectral decomposition components do not highlight gas anomalies in the oil zone, the use of a combined attribute response — involving the specific 18 Hz spectral component rotated by -90 degrees, together with 4D Acoustic Impedance (IP4D) — shows good correlation with the variation in gas saturation observed in the vicinity of the well. This methodology, also enhanced by geobody generation to isolate anomalies, improves the detection of subtle variations associated with water-alternating-gas (WAG) injection cycles in complex carbonate settings, thereby supporting long-term reservoir management.

Keywords: frequency-phase analysis; inversion seismic; time-lapse; 4D

INTRODUCTION

It is well known that 4D seismic is very challenging in carbonate reservoirs (Cruz et al., 2021). This is because these carbonates are stiff and typically less porous than sandstones, making the impedance changes due to the production effect to be very subtle (Cypriano et al., 2019). In the case of the Mero field, located in the Brazilian pre-salt Santos Basin, whose development strategy includes, among other tools, the total reinjection of produced gas and frequent water-alternating-gas (WAG) injection cycles, a high quality, repeatable and frequent 4D monitoring becomes an essential tool for reservoir management.

To better quantify the specific 4D challenges of Mero, a synthetic seismic dataset was generated from full wave elastic modeling using elastic Tilted Transverse Isotropy (TTI) property models that

encompasses not only the reservoir layers but also the overburden and basement. Different survey geometries were considered for baseline and monitor vintages, by using the pre-plot and post-plot results of the shot and receiver positions from the baseline 2018 3D Nodes acquisition, so that geometric repeatability noise could be accounted for. By allowing these geometry misfits to occur in either source only, or source and receiver locations, both Nodes and Permanent Reservoir Monitoring (PRM) scenarios were investigated. The synthetic data was processed using an in-house Least-Squares Reverse Time Migration (LSRTM) algorithm and the results were compared to real 3D Ocean Bottom Nodes (OBN) data, providing confidence in the usability of the synthetics.

Studies carried out from the synthetic data show that the main challenge of the Mero 4D project is to detect gas saturation changes in the oil zone, since its fluid presents high gas-oil ratio (GOR) and CO_2 content, resulting in a low impedance contrast of 0.5-1% dIp/Ip between in situ fluid and reinjected gas. In addition, cumulative changes of injected fluid can produce a destructive combination of effects leading the 4D signal to almost disappear. Lastly, the large initial depletion expected over the first years of production appears to further mask the amplitude related to gas saturation effects. Due to this combination of factors, the sensitivity of the final interpretability of the 4D signal to even small amounts of 4D noise are shown to be critical, and very low Normalized Root Mean Square (NRMS) values are therefore required.

Aiming to support this challenging task, the spectral decomposition technique (Partyka, 2005) was tested by Grochau and Jilinski (2016) on synthetic data generated through a representative geological model and in a dynamic property flow simulator. The results of this work showed, among other things, that the spectral decomposition data exhibited good correlation with water saturation variation. However, variations in pressure and gas saturation remained challenging, as observed with amplitude data.

The objective of this work was to extend the studies mentioned above, aiming to analyze not only the behavior of the frequency component but including phase response and amplitude in terms of its acoustic component of the 4D signal in the vicinity of an injector well in the field. For this purpose, synthetic seismograms generated from simulations of the injection data from this well at different dates were used, and an innovative methodology for 4D signal analysis was applied, based on the attribute generated through the correlation response among the components of spectral decomposition and 4D acoustic inversion. Finally, the integrated response was extracted as a geobody highlighting the verified spatial correlation among physical properties and the calculated attributes. Understanding how the gas front moves throughout the reservoir, especially in the oil zone, is essential to increase the recovery factor in fields such as Mero, which employs a strategy of total reinjection of produced gas and has platforms limited by gas processing capacity.

STUDY AREA

The Mero field is one of the largest hydrocarbon discoveries in Brazil, with an estimated volume between 8 and 12 billion barrels of oil equivalent (BOE). It is located in the northeastern Santos Basin, offshore southeastern Brazil.

The basin is associated with the breakup of Gondwana during the Early Cretaceous and features a

complex stratigraphy, commonly divided into pre-salt, salt, and post-salt domains (Figure 1). The pre-salt section includes the reservoir, located at depths ranging from 5.000 to 6.000 meters, and is composed of carbonate rocks from the Itapema Formation (mainly coquinas) and the Barra Velha Formation (grainstones and stromatolitic textures) (Moreira et al., 2007).

Stratigraphically, the Barra Velha Formation is subdivided into two subunits: Upper Barra Velha (BVE100 and BVE200) and Lower Barra Velha (BVE300).

Overlying the reservoir is the evaporitic seal unit, referred to here simply as "salt," composed mainly of halite and anhydrite from the Ariri Formation (Late Aptian) (Moreira et al., 2007). The post-salt sequence comprises the Guarujá, Itanhaém, Itajaí-Açu, and Marambaia formations, generally characterized by carbonates, sandstones, and shales.

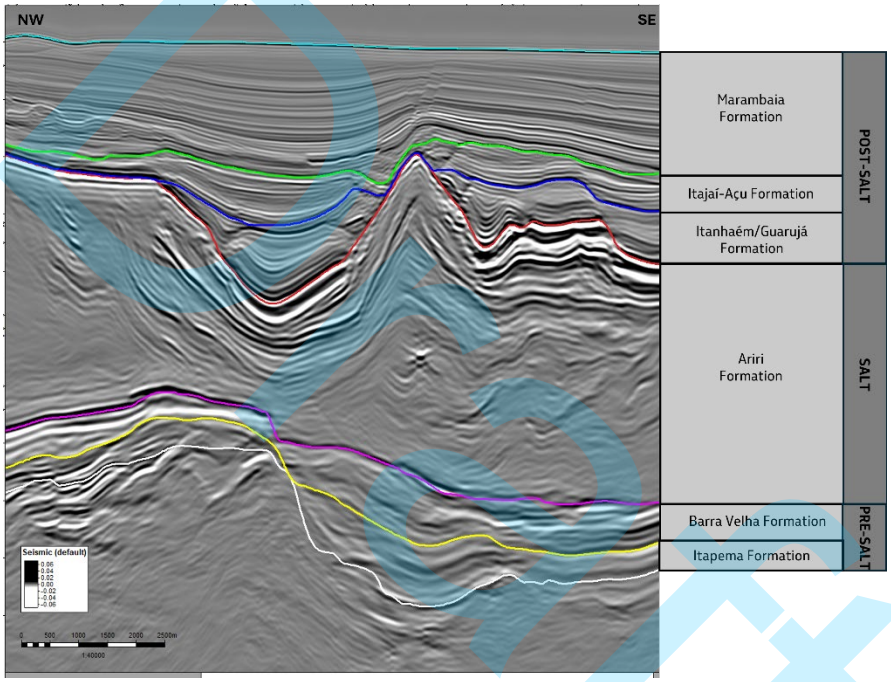

Figure 1 - Arbitrary section indicating post-salt, salt and pre-salt domains, with respective geological formations.

METHODOLOGY

To better understand the amplitude-frequency anomalies effects on 4D seismic data, this study focused on the vicinity of a WAG (water-alternating-gas) injection well in a pre-salt reservoir field. Synthetic Base and Monitor seismograms were generated, with the analysis restricted to the well's location to ensure detailed evaluation.

Model Construction and Data Integration

The synthetic seismic volumes were developed through advanced modeling, incorporating multiple data sources for regions outside the reservoir, such as well logs, Kirchhoff and RTM (Reverse Time Migration) migrated data, FWI (Full Waveform Inversion) velocity models, and tomographic attributes (Epsilon, Delta, Intercept, and Gradient).

The initial step involved creating a hybrid "KIRTM" dataset by merging the Kirchhoff and RTM

stacked volumes, followed by illumination corrections. This hybrid dataset provided the high-frequency component of the impedance model using the Iterdec® approach (Cunha et al., 2019). The high-frequency information was then integrated with the FWI-derived low-frequency, Vp velocity and initial density volumes, resulting in a full-band impedance model. To further enhance resolution, AVO (Amplitude versus Offset) attributes were incorporated. Velocity variations (dVp/Vp and dVs/Vs), derived from Intercept and Gradient, were calibrated using sonic Vp and Vs records from the sole pilot well in the post-salt interval (Deplante et al., 2019). For the reservoir, conventional petro-elastic modeling, based on concepts of Gassmann (1951) and validated by Vasquez et al. (2019) for the Brazilian pre-salt conditions, was performed, generating Vp, Vs, and density volumes based on flow model information. Figures 2, 3 and 4 illustrate the final volumes utilized in elastic modeling.

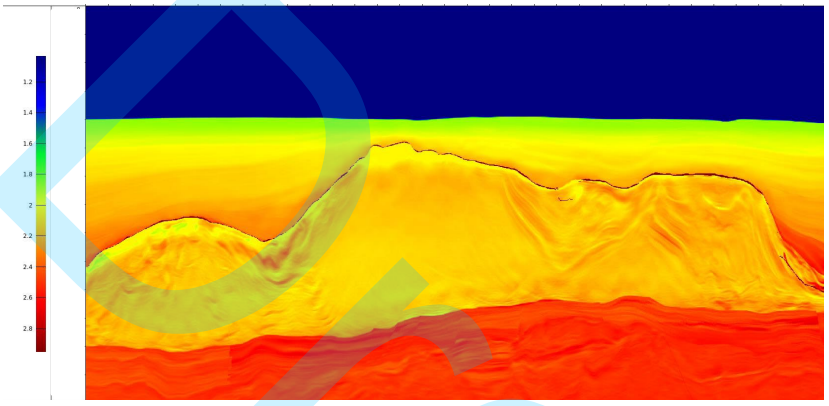

Figure 2 – Arbitrary section of density, showing the contrast among post-salt, salt and pre-salt zones.

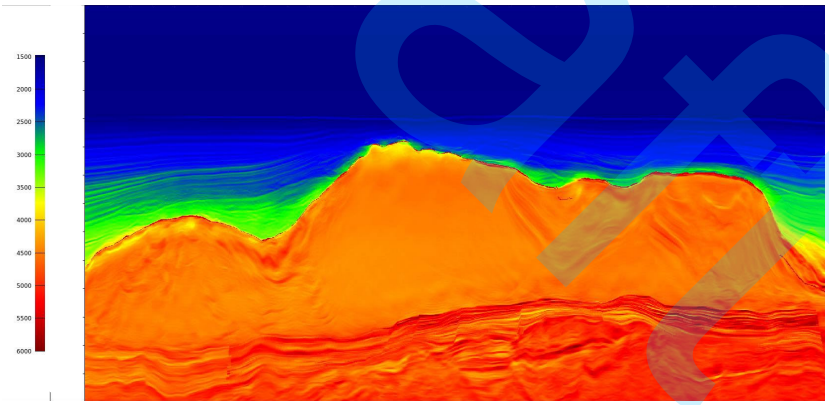

Figure 3 – Arbitrary section of P-velocity, showing major contrast among post-salt and salt/pre-salt zones.

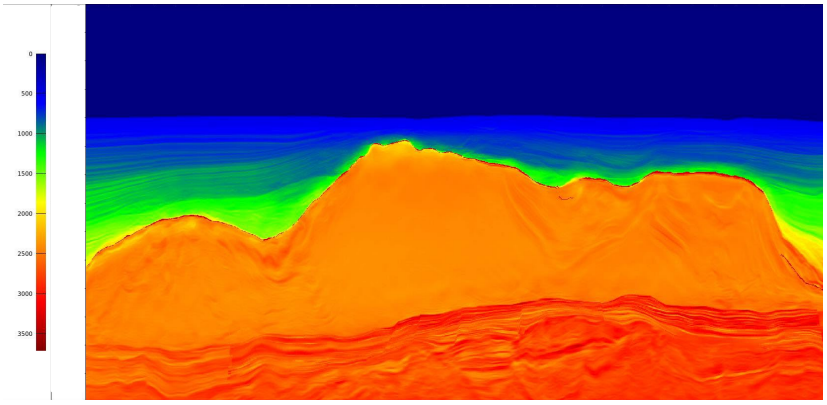

Figure 4 – Arbitrary section of S-velocity, showing major contrast among post-salt and salt/pre-salt zones.

Using this refined model, synthetic acquisition scenarios were generated for the Base (Jan/2016) and Monitor (Jan/2025) surveys. The data was processed and imaged with LSRTM (Least-Squares Reverse Time Migration; Wang et al., 2017), yielding migrated volumes that served as the foundation for this analysis (Figures 5 and 6).

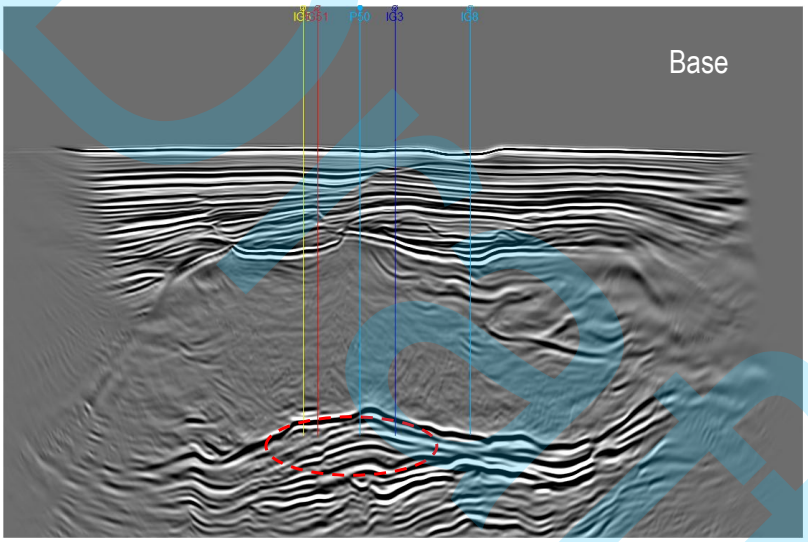

Figure 5 – LSRTM arbitrary seismic section from Base survey intercepting injector (IG3, IG5, IG8, IG51) and producer wells (P50). The red dotted line represents the area of interest in the pre-salt reservoir reached.

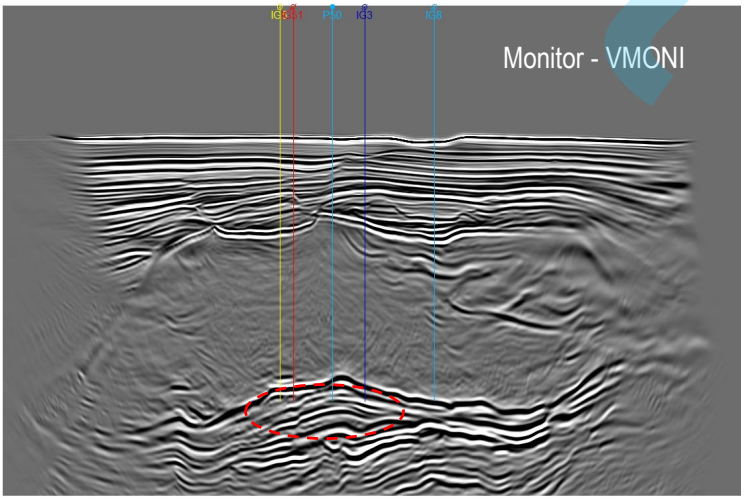

Figure 6 – LSRTM arbitrary seismic section from Monitor survey intercepting injector (IG3, IG5, IG8, IG51) and producer wells (P50). The red dotted line represents the area of interest in the pre-salt reservoir reached.

Generalized Spectral Decomposition (GSD) and 4D acoustic inversion response integration methodology

To apply Generalized Spectral Decomposition, the frequency spectra of the Base and Monitor seismic datasets were examined, focusing on amplitude distribution with respect to frequency (Castagna et al., 2003; Grochau and Jilinski, 2016). The analysis was confined to the well location, enabling the identification of subtle frequency anomalies, which may otherwise be undetectable at the field scale.

Based on the spectrum analysis (Figure 7), three frequency components were selected: 9 Hz, 18 Hz (peak frequency) and 26 Hz. Additionally, phase parameterization was performed, generating equally spaced volumes at -180º, -90º, 0º, +90º and +180º for each frequency (Castagna et al., 2016).

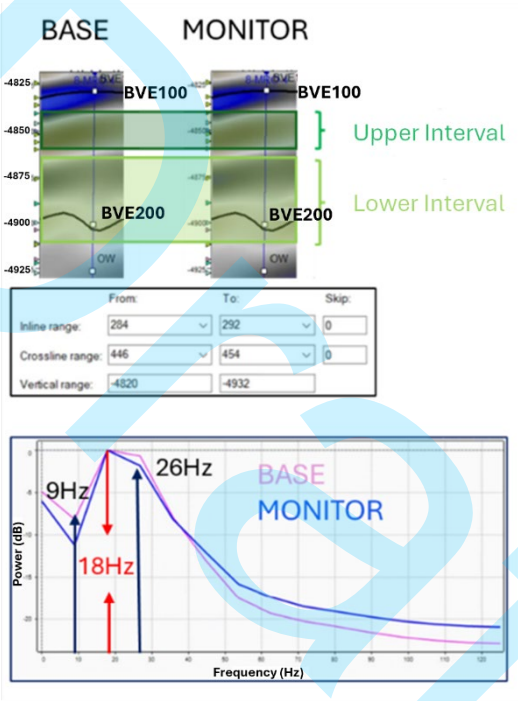

Figure 7 – The frequency spectrum, extracted from the internal intervals above, shows a reduction in low-frequency content (around 9 Hz) in the Monitor volume, while an increase is observed in the high-frequency range compared to the Base volume.

GSD attributes were extracted following these parameterizations, and the difference between corresponding frequency components for each phase was calculated: DIFF GSD = GSD_MONITOR – GSD_BASE (Figure 8). This approach aimed to investigate how spectral components correlate with 4D amplitude anomalies.

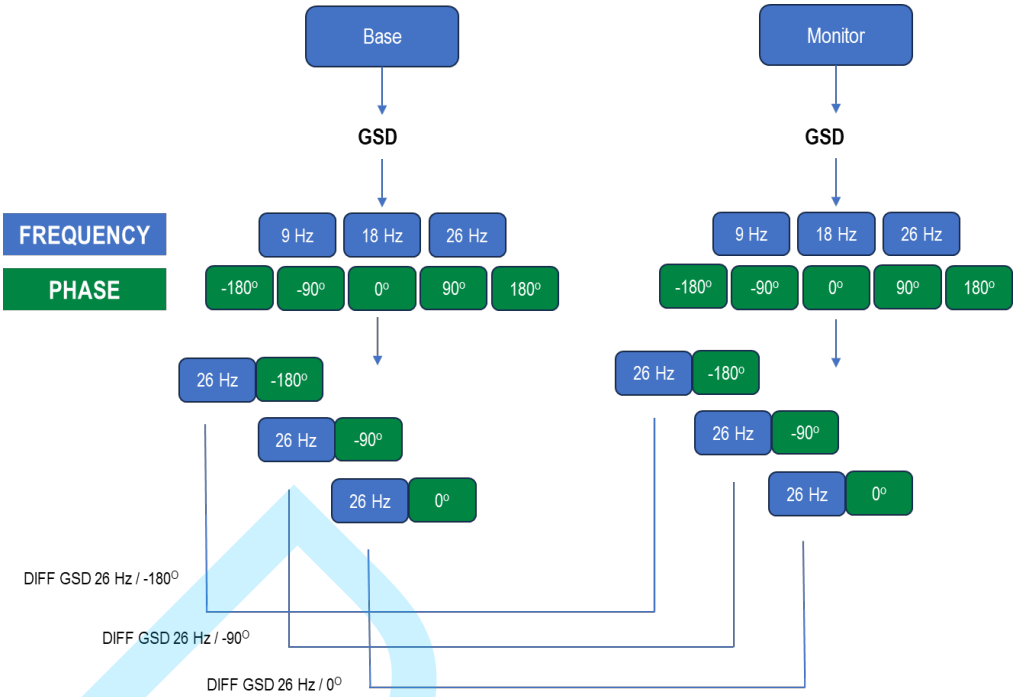

Figure 8 – Methodology used to create the 4D GSD volumes as a function of frequency content and phase rotation.

The results from spectral decomposition were further integrated with the 4D Acoustic Impedance Volume (IP4D), representing impedance variations between Base and Monitor surveys. This combination was motivated by the direct relationship between impedance and rock properties, enhancing the identification of saturation change anomalies, as discussed by Matto Grosso da Silva et al. (2024). For the study well, the WAG injection is mainly defined by BVE100 interval.

By employing advanced modeling techniques and integrating multiple seismic attributes, this workflow enables a detailed assessment of how spectral and amplitude variation affects 4D seismic response. The methodology enhances the detection of subtle amplitude and frequency anomalies related to reservoir changes and provides a robust framework for linking seismic responses to physical property variations, thereby supporting more effective reservoir monitoring in complex pre-salt environments.

RESULTS AND DISCUSSION

The results of this study are illustrated in Figures 9, 10 and 11, which present the GSD attributes extracted as previously described, along with their respective differences for the frequencies of 9 Hz, 18 Hz and 26 Hz, and for the phase components of -180º, -90º, 0º, +90º, and +180º. These figures provide a comprehensive overview of the spectral decomposition analysis performed.

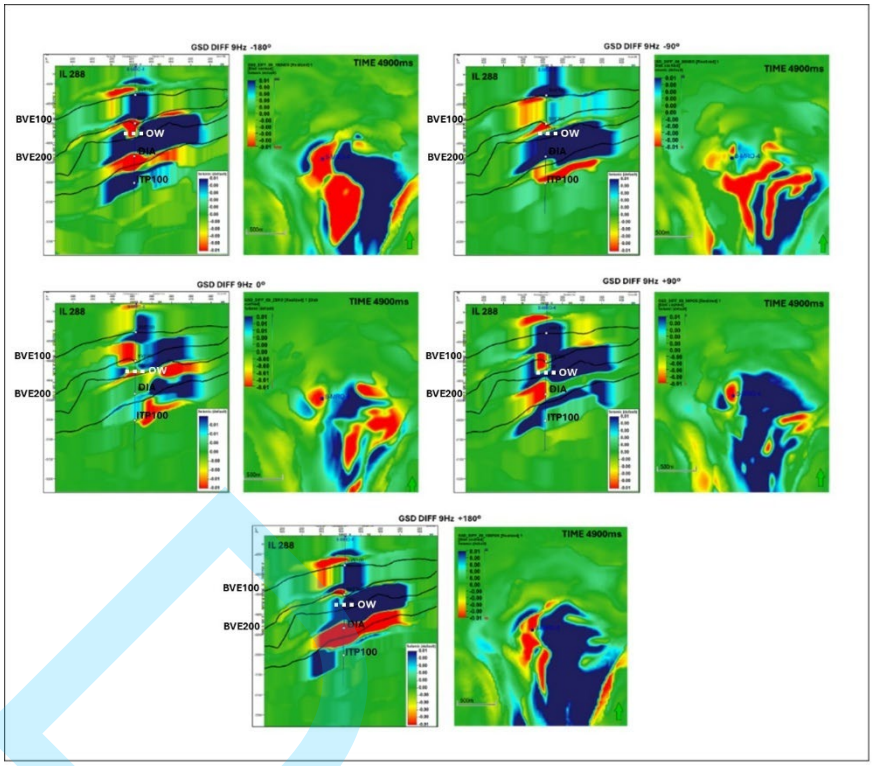

Figure 9 – GSD attributes extracted from the Base and Monitor Volumes with a central frequency of 9 Hz, varying only the operator phase, along Inline 288 and time slice 4900 ms.

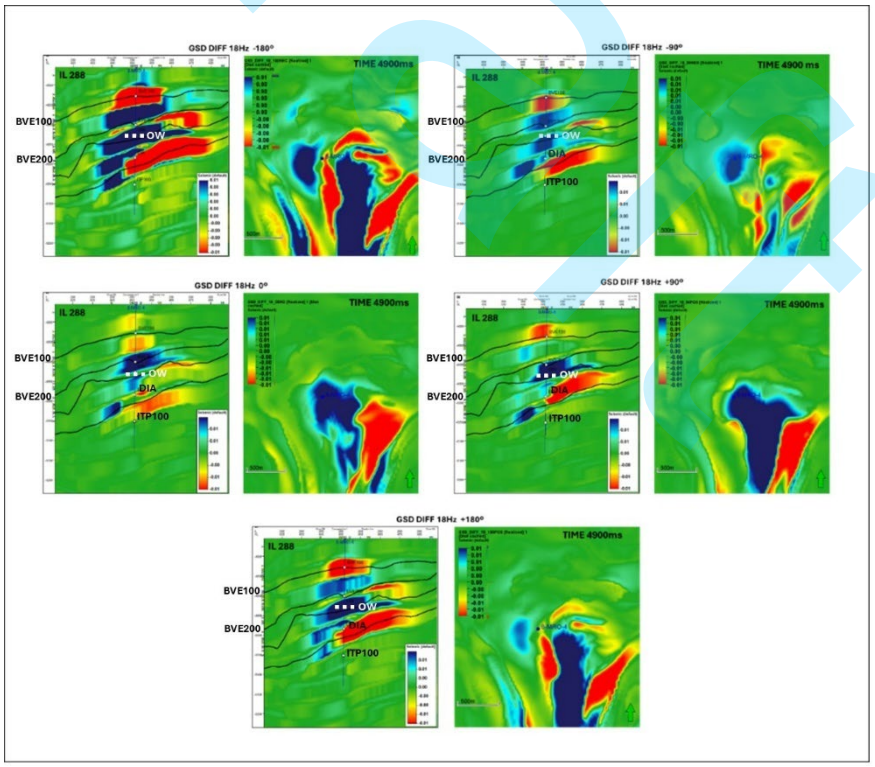

Figure 10 – GSD attributes extracted from the Base and Monitor Volumes with a central frequency of 18 Hz, varying

only the operator phase, along Inline 288 and time slice 4900 ms.

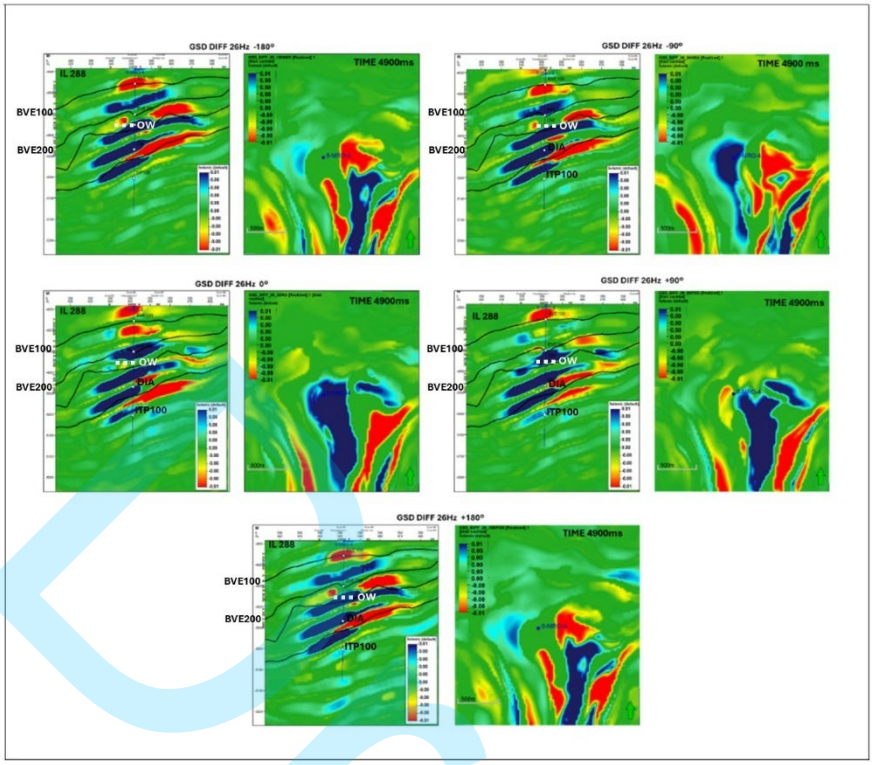

Figure 11 – GSD attributes extracted from the Base and Monitor Volumes with a central frequency of 26 Hz, varying only the operator phase, along Inline 288 and time slice 4900 ms.

The outcomes are particularly noteworthy, as they reveal a progressive improvement in vertical resolution—most evident in the BVE200 interval, where some reflectors are better resolved in the frequency domain. As anticipated, the resolution increases with frequency: the GSD 9 Hz volume displays low vertical resolution, whereas the GSD 26 Hz volume achieves the highest vertical resolution among the tested components. This observation underscores the importance of frequency selection in enhancing seismic resolution in complex carbonate settings.

Although these results are consistent with theoretical expectations, it is important to note that the frequency attribute, even when combined with phase, does not fully resolve the challenge of detecting and highlighting gas anomalies within the oil zone. This finding suggests that additional information or integration of other attributes may be necessary to address the complexity of fluid substitution effects in the reservoir.

To further investigate this, Figure 12 presents the inversion response superimposed on the measured impedance log, resampled to 4 ms for quality control in both scenarios. This figure also demonstrates that the same resampled log can be cross-validated with curves extracted from the low-frequency model and the seismic inversion response at the well location, providing a robust framework for quality control.

From Figure 12, it is evident that the model exhibits a reasonable correlation between the seismic inversion and the well log response, successfully capturing the overall trend of the acoustic impedance measured throughout the well.

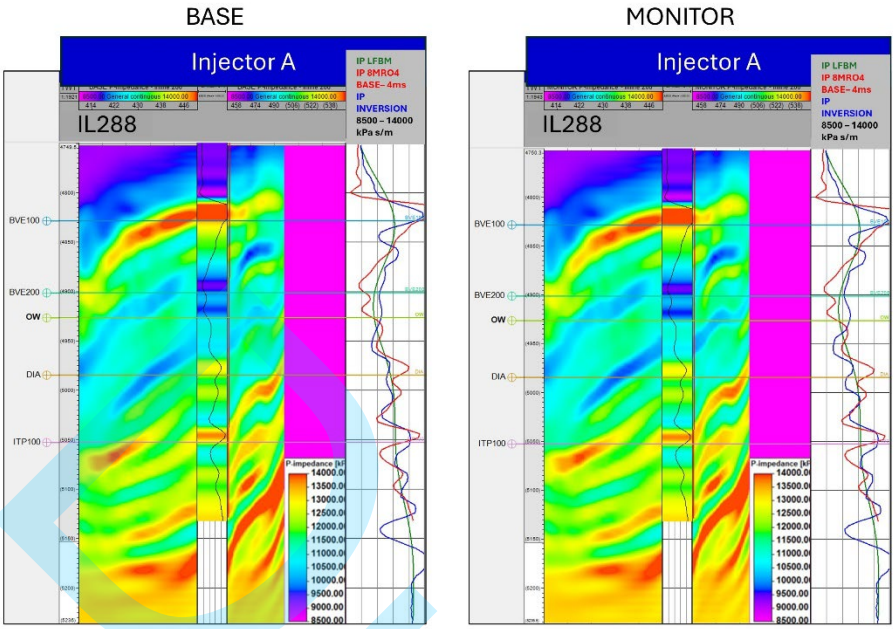

Figure 12 –Acoustic Impedance volumes over Impedance log resampled to 4ms. Red curve represents well impedance; blue curve describes model impedance; and green curve is model impedance smoothed.

The acoustic impedance calculated by the inversion can also be evaluated in a sectional view, as shown in Figure 13. This figure displays the acoustic impedance for both scenarios, along with the IP4D, which represents the key parameter of interest in this 4D seismic inversion workflow. Analysis of the percentage variation of IP, called IP4D property reveals a percentage increase in impedance (hardening) near the top of the Barra Velha Formation and a subtle percentage decrease in impedance (softening) at the base of the same interval. The hardening anomaly corresponds to an oil-to-water substitution, reflecting a period of water injection and increased water saturation near the well. Since water has a higher density than oil, an impedance increase is expected in this region. Conversely, for oil-to-gas substitution, impedance decreases due to the lower density of gas, resulting in the observed softening effect at the base of the Barra Velha interval. These two effects are fully consistent with the expected anomalies, considering the well under study operates in a WAG injection mode, alternating between water and gas injection and generating both types of anomalies in its vicinity.

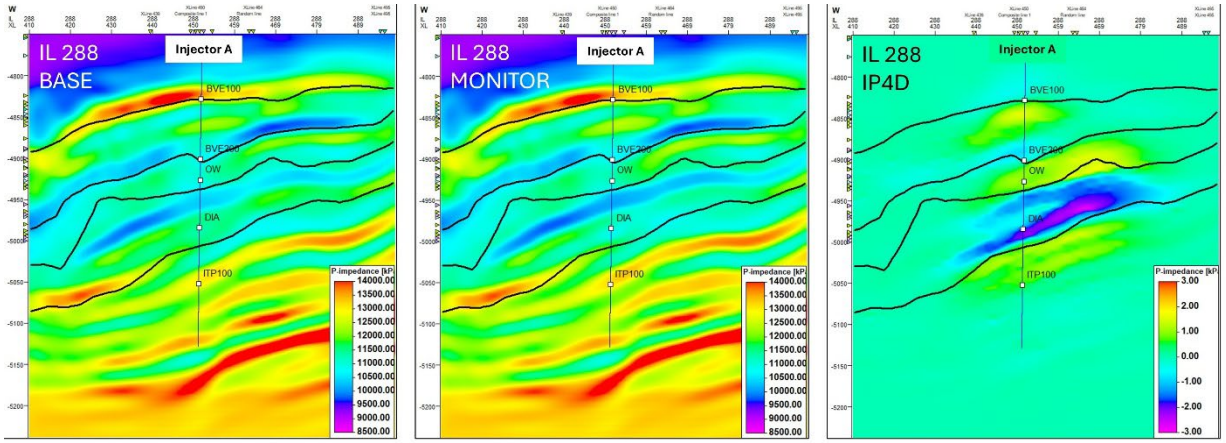

Figure 13 – Seismic section showing the calculated acoustic impedance for both scenarios and the IP4D.

Although the main focus is the BVE interval, it is also important to highlight the strong negative response (softening) detected in the Intra-Alagoas unconformity (DIA) interval, which is clearly visible in both the seismic data and previously calculated attributes. This anomaly appears to be associated with gas injection into the aquifer. However, since such a strong anomaly was not anticipated given the relatively small saturation variation in the region, further investigation is warranted.

To establish potential correlations and patterns, various property data at the well location were compiled, enabling an integrated analysis that could be extended to the entire volume. The comprehensive figure below presents the well responses for the measured IP, the variation in IP calculated from the inversion (IP4D), the differences in instantaneous phase (DIFF INST PHASE) and instantaneous frequency (DIFF INST FREQ), the variation in water and gas saturation (SW and SG), the variation in pore pressure (PP), and the spectral decomposition difference attributes for 9 Hz, 18 Hz and 26 Hz (DIFF GSD), grouped by operator phase (90º, -90º, 0º, -180º and 180º). The possible zones of interest—upper, intermediate and lower reservoir—are also highlighted in Figure 14.

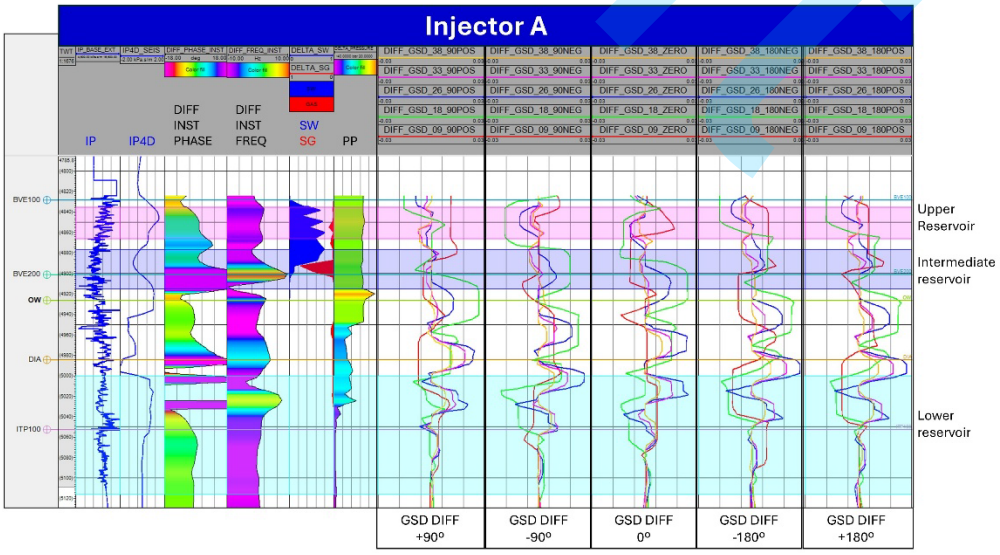

Figure 14 – Well data showing measured IP, IP4D, phase variations, frequency, saturation, pressure, and spectral differences. Includes zones of interest in the reservoirs.

This integrated analysis reveals that IP variation responds directly to saturation changes within the BVE100 interval, indicating hardening with increased water saturation and softening associated with the gas peak at the base of the interval. Notably, the instantaneous phase and frequency attributes display strong anomalies corresponding to this gas saturation peak. For pore pressure variations, a decrease is observed in the phase and frequency difference attributes, particularly in the frequency attribute; however, impedance itself does not show a specific response to pressure changes. When examining the spectral decomposition attributes, it is evident that operators with phase +180º and -180º do not show direct relationships to the model variations.

A more detailed examination of the 18 Hz frequency component with +90º and -90º phase reveals a direct relationship with changes in water and gas saturation, responding inversely in the regions where these occur (upper and intermediate reservoirs). While the positive phase component follows the IP4D trend, the negative phase component exhibits opposite behavior. In regions with minimal saturation variation, both behave similarly, except at the oil-water contact (OWC), where the -90º phase component shows a pronounced peak. This sensitivity to saturation changes highlights the potential value of this attribute in reservoir monitoring, as further illustrated in Figure 15.

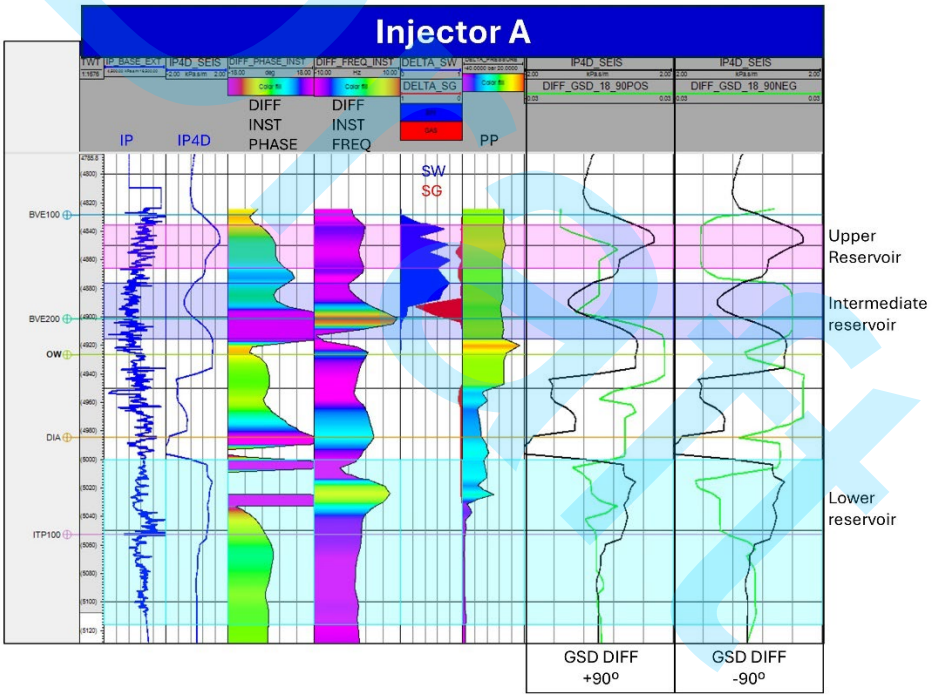

Figure 15 – 18 Hz components (+90º and -90º) in relation to IP4D.

With respect to pressure variation, most attributes do not show an obvious relationship, only subtle indications. The most significant effect is a slight decrease in the DIFF_GSD_18_-90º attribute, as seen in the instantaneous frequency variation. Through this cross-analysis of seismic attribute and impedance responses at the well, it becomes clear that the combination of impedance variation and the DIFF_GSD_18_-90º attribute can effectively help delineate water and gas fronts.

Consequently, it becomes necessary to generate a combined attribute that integrates the response of

the spectral decomposition component with the 4D acoustic impedance property. Despite the clear correlation at well location, it is not simple to analyze the spatial correlation of these attributes. To support this understanding the volumetric response of both attributes were analyzed and constrained through its spatial distribution having in mind the anomaly along the well. The use of geobodies proves to be an effective approach for integrating of both attribute and facilitates the interpretation of gas anomalies. Based on the results described above, geobodies were constructed from the attribute that combines IP4D with GSD, using response thresholds identified at the well (GSD_DIFF_18_90NEG > 0.11 and < 0.21).

Figure 16 presents the geobodies of the combined attribute together with those from the gas saturation model, enabling assessment of their spatial distribution. The combined attribute shows good correlation with gas saturation variation near the well, and the geobodies derived from it are more continuous than those from the saturation model, which can be attributed to the higher resolution of the seismic-scale attribute (typically 12.5 m x 12.5 m) compared to the reservoir engineering model (100 m x 100 m).

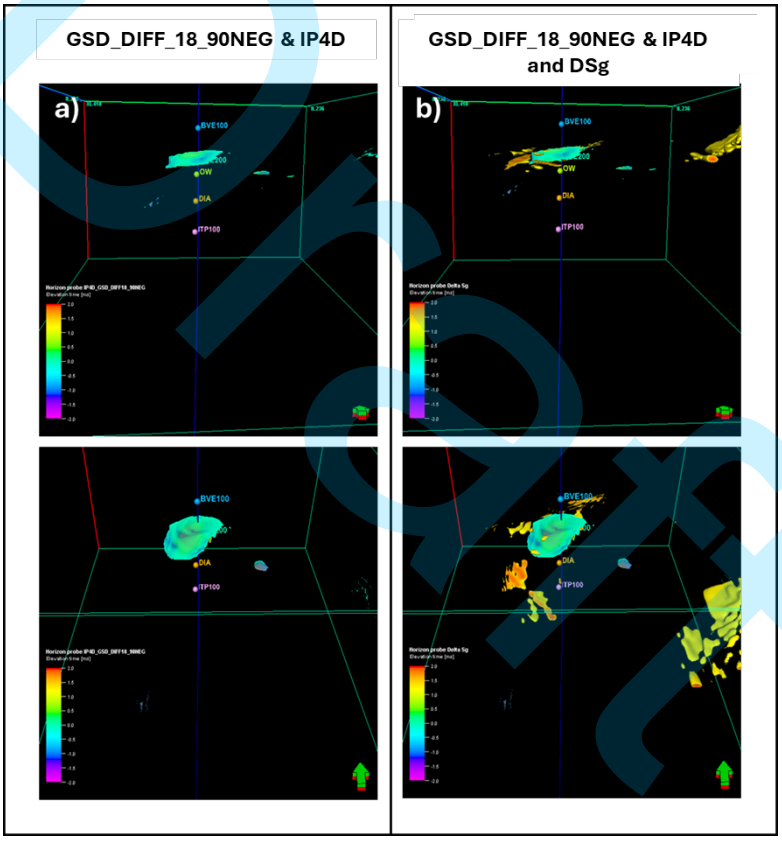

Figure 16 – a) Geobodies isolated from the combined response of the GSD_DIFF_18_90NEG & IP4D attribute and b) the visualization of this attribute with the delta gas saturation (DSg) attribute.

Building on this, a seismic volume can be generated from the geobodies, providing a focused visualization of the amplitude related solely to the anomaly captured by the combined attribute. Figure 17 presents the converted seismic volume from the probe generated using the parameterization of the GSD_DIFF18_90NEG and IP4D volumes, with normalized values for these properties.

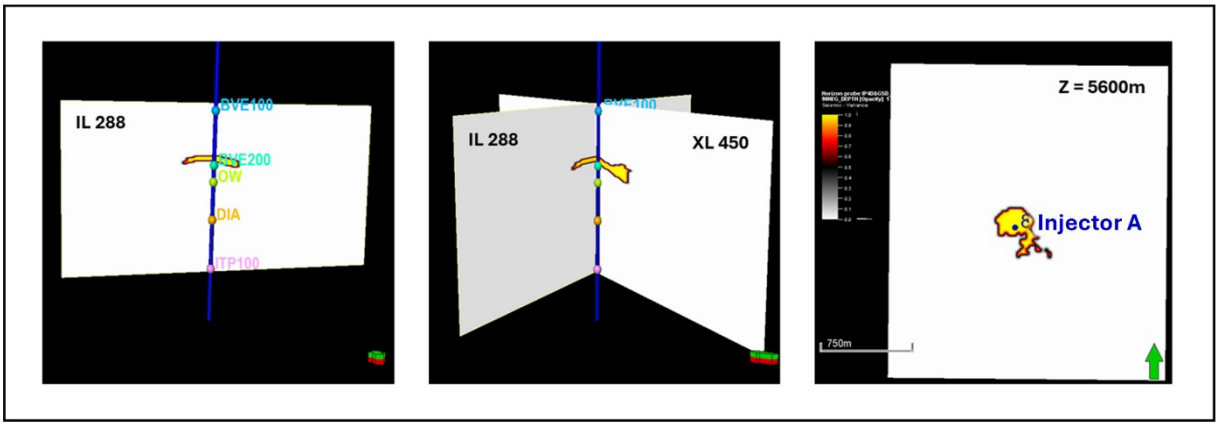

Figure 17 – Geobodies converted to seismic volume assuming the values of the normalized input volumes (GSD_DIFF18_90NEG and IP4D) for this new property.

Finally, by integrating the converted geobodies with other available project volumes, the consistency of the results can be thoroughly assessed. Figure 18 demonstrates this integration, showing the seismic volume generated from the geobodies superimposed on the 4D volume (DIFF_MONI-BASE) and the saturation model response (SG) at the well. This comparison reveals an excellent correlation between the newly created attribute and the other properties analyzed, confirming the robustness of the proposed methodology.

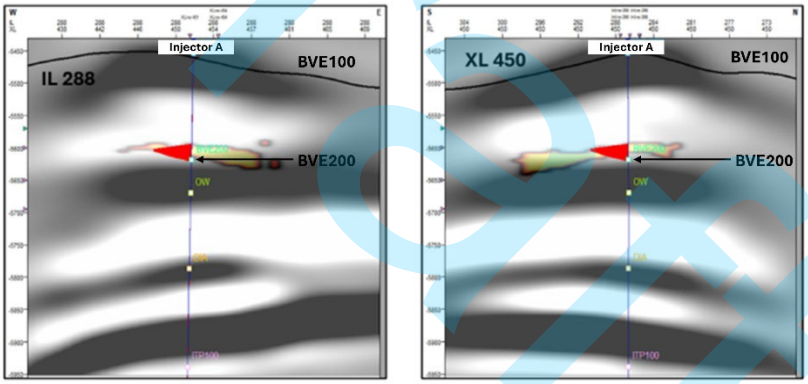

Figure 18 – Attribute created from the converted Geobodies, overlaid with the 4D seismic response and the SG model anomaly at the well position.

CONCLUSIONS

This work addresses a significant challenge faced in giant Brazilian pre-salt fields: detecting variations in gas saturation within the oil zone of pre-salt carbonate reservoirs. The identification and mapping of such anomalies are particularly demanding due to the rigidity of the rock matrix and, especially, the low contrast between reinjected gas and in-situ fluids—an issue that becomes even more critical in fields with high CO_2 content, such as the Mero field.

To this end, synthetic models and seismograms were developed using advanced modeling techniques that simulated injection well scenarios across different acquisition dates. This enabled the application of an innovative methodology for 4D signal analysis, centered on spectral decomposition and

seismic inversion to create a combined attribute derived from both properties. The spectral decomposition process, implemented via the Generalized Spectral Decomposition (GSD) methodology, allowed for the extraction of various combinations of frequency and phase components from the seismic data. Selection of the most relevant frequency components was guided by a detailed analysis of the Base and Monitor datasets' spectra. In addition to the peak frequency at 18 Hz, frequencies showing the greatest spectral contrast (9 Hz and 26 Hz) were chosen for further analysis. The phase components considered included: 180º, -90º, 0º, +90º, and +180º.

Upon analyzing the volumes generated for each frequency and phase combination in relation to the saturation and pressure models, it became clear that the spectral decomposition attribute alone was insufficient to fully address the objectives of the study. This finding pointed to the need for integrating additional information to enhance anomaly detection.

Consequently, 4D Acoustic Impedance (IP4D) was incorporated into the workflow. While IP4D is strongly linked to variations in rock properties, in the context of this study, it showed a closer correlation with changes in water saturation than with gas saturation. A more focused analysis around the studied well area revealed a strong correlation between the 18 Hz frequency component with a -90º operator rotation, the IP4D, and the observed variations in gas and water saturation. This insight motivated the generation of a combined attribute, integrating these frequency and phase components with IP4D.

Subsequently, this targeted seismic response was compared to the saturation variation model, with particular attention to the curve at the well location. The comparison demonstrated a strong correlation between the response of seismic attribute derived from the geobodies and the gas saturation variation curve at the well. This result underscores the promise of the proposed methodology and attribute for identifying gas anomalies in the oil zone, even when those anomalies are of very low amplitude.

The findings from this study pave the way for future research and applications. One recommended next step is to investigate the behavior of the combined attribute across the entire seismic volume, with the aim of identifying even weaker anomalies that may not be contiguous with those near the well. Such anomalies are anticipated, given that pre-salt fields typically feature numerous WAG wells, which alternate between gas and water injection. As a result, isolated gas fronts with low saturation variation are likely to exist, gradually dissipating within the reservoir. Detecting these subtle anomalies is crucial, as they reveal fluid pathways, assist in identifying geological heterogeneities, and support the calibration of gas breakthrough timing in producer wells.

Finally, further investigation is warranted regarding the pronounced anomaly observed in the 4D data within the aquifer zone. This anomaly remains difficult to explain, considering the small gas saturation variation predicted by the models, and represents an intriguing avenue for future study.

ACKNOWLEDGMENTS

The authors would like to thank all the colleagues that contributed to this work, SLB for the technical and scientific support also software access and the Libra JPT partners (Petrobras, TotalEnergies, Shell Brazil, CNPN. CNOOC Limited and PPSA) for the permission to publish these results.

REFERENCES

Castagna, J. P.; S. Sun; R. W. Siegfried. Instantaneous spectral analysis: Detection of low-frequency shadows associated with hydrocarbons: The Leading Edge, 22, 120–127, 2003. DOI: 10.1190/1.1559038.

Castagna, J.; Oyem, A.; Portniaguine, O.; Aikulola, U. Phase decomposition. Interpretation 4, SN1–SN10, 2016. DOI: 10.1190/INT-2015-0150.1.

Cypriano, L., Yu, Z., Ferreira, D., Huard, B., Pereira, R., Jouno, F., Khalil, A., Urasaki, E., da Cruz, N., Yin, A., Clarke, D., Jesus, C. OBN for pre-salt imaging and reservoir monitoring –Potential and road ahead. In: Sixteenth International Congress of the Brazilian Geophysical Society, 2019, Rio de Janeiro, Brazil. DOI: 10.22564/16cisbgf2019.318.

Cunha, C. A.; Damasceno, A.; Pimentel, A. L.; Silva, L. M. T.; Cruz, N. M. S. M.; Oliveira, T. A. S. High resolution impedance inversion. Brazilian Journal of Geophysics, v. 37, n. 4, p. 461-469, 2019. DOI: 10.22564/rbgf.v37i4.2022.

Cruz, N. M.; Cruz, J. M.; Teixeira, L. M.; Costa, M. M.; Oliveira, L. B.; Urasaki, E. N.; Bispo, T. P.; Jardim, M. S.; Grochau, M. H.; Maul, A. Tupi Nodes pilot: a successful 4D seismic case for Brazilian presalt reservoirs. The Leading Edge, v. 40, n. 12, 886-896, 2021. DOI: 10.1190/tle40120886.1.

Deplante, C.; Costa, M.; Santos, M. S.; Dias, R.; Mello V.; Meirelles, B. R.; Araujo, S. S.; Garcia, D. C.; Sansonowski, R. Using full wave seismic modeling to test 4D repeatability for Libra pre-salt field. In: International Congress of the Brazilian Geophysical Society (SBGf), 16., 2019. Rio de Janeiro, Brazil. DOI: 10.22564/16cisbgf2019.343.

Gassmann, F. On Elasticity of Porous Media, in Classics of Elastic Wave Theory. Geophysik, Zürich, v. 17, p. 1-23, 1951.

Grochau, M.; Jilinki, P. 4D seismic spectral decomposition over a presalt carbonate reservoir: a feasibility study. In: SEG Technical Program Expanded Abstracts 2016. Society of Exploration Geophysicists, 2016. DOI: 10.1190/segam2016-13870124.1.

Matto Grosso da Silva, C. J.; Benac, P.; Botelho, E.; Mucelini, H.; Lima, R.; Santos, P. F.; Garcia, M. A.; Camanho, T.; Pedrosa, C. A. Integrating 4D seismic interpretation and water saturation estimation in the well reposition: applications in Marlim Field, Campos Basin, Brazil. Brazilian Journal of Geophysics. v. 42, n. 3, 2024. DOI: 10.22564/brjg.v42i3.2331.

Moreira, J. L.; Madeira, C. V.; Gil, J. A.; Machado, M. A. P. Bacia de Santos. Boletim de Geociências da Petrobras, n. 15 (2). p. 531-549, 2007.

Partyka, G.; Spectral Decomposition and Spectral Inversion. In: SEG Spring 2005 Distinguished Lecture. 2005. DOI: 10.1190/e-learning_20060131.

Vasquez, G. F.; Morchbacher, M. J.; Justen, J. C. R. Experimental efforts to access 4D feasibility and interpretation issues of Brazilian presalt carbonate reservoirs. Interpretation, v. 7, n. 4, p. SH1-SH18, 2019. DOI: 10.1190/int-2018-0203.1.

Wang, P.; Huang, S.; Wang, M. Least-squares RTM: Theory and applications. In: International Congress of the Brazilian Geophysical Society (SBGf), 15., 2017. DOI: 10.1190/sbgf2017-238.